

1 Supporting Information

2  
3 **Condensational Uptake of Semivolatile Organic Compounds in Gasoline**  
4 **Engine Exhaust onto Pre-existing Inorganic Particles**

5  
6 Shao-Meng Li\*, John Liggio, Lisa Graham<sup>1</sup>, Gang Lu, Jeffrey Brook, Craig Stroud,  
7 Junhua Zhang, Paul Makar, Michael D. Moran

8  
9 Air Quality Research Division, Atmospheric Science and Technology Directorate,  
10 Science and Technology Branch, Environment Canada  
11 4905 Dufferin Street, Toronto, Ontario M3H 5T4, Canada

12  
13 <sup>1</sup> 335 River Road, Ottawa, Ontario, K1A 0H3 Canada (now at Department of Chemistry,  
14 University of Christchurch, Canterbury 8041, New Zealand)

15  
16 For submission to *Atmospheric Chemistry and Physics*

17  
18 Revised Version: May 31, 2011

19  
20  
21  
22 **AURAMS Description**

23  
24 AURAMS (version 1.4.0) is an off-line chemical transport model (CTM) that is  
25 driven by the Canadian operational weather forecast model, GEM (Global Environmental  
26 Multiscale model). GEM (version 3.2.2) was used to produce meteorological fields with a  
27 15-km horizontal grid spacing. GEM was run for 12-hr periods from reanalysis files with  
28 a 6-hr spin-up and 6-hr of simulation stored for the CTM. AURAMS was run with a 15-  
29 km horizontal grid spacing for a domain covering the northeastern U.S. and eastern  
30 Canada and using climatological chemical boundary conditions.

31 Gridded hourly anthropogenic point, area and on-road mobile emissions files were  
32 prepared for the CTM with the 2005 Canadian and 2005 U.S. national criteria-air-  
33 contaminant emissions inventories and version 2.2 of the SMOKE emissions processing  
34 system. Total gasoline exhaust organic vapour was treated as an additional gas-phase  
35 species in the on-road mobile emissions stream of the emissions processing system. This  
36 species was emitted, transported, lost by gas-phase chemistry and allowed to reach an  
37 equilibrium partitioning with sulphate aerosol based on the effective uptake coefficient fit

---

\* Corresponding author; [shao-meng.li@ec.gc.ca](mailto:shao-meng.li@ec.gc.ca); 1-416-739-5731

38 of Equation (6) ( $S=0.012+0.000137*THC^{2.53}$ ) where uptake has units of kg organic  
39 particle per kg sulfate and GTHC has units of  $\mu\text{g m}^{-3}$ ). A Newton iteration method was  
40 used to calculate the equilibrium solution with a 1% convergence criteria for the GTHC  
41 vapour. Gas-phase loss by oxidation with OH, NO<sub>3</sub> and O<sub>3</sub> was calculated with rate  
42 coefficients of 1.2E-11, 1.2E-14 and 6.7E-18 cm<sup>3</sup> molec<sup>-1</sup> sec<sup>-1</sup>, respectively. These rate  
43 coefficients are reactivity-weighted averages from the individual species rate coefficients  
44 in the VOC emissions profile for gasoline exhaust.

45 Gasoline exhaust primary organic aerosol emissions were also modelled in  
46 AURAMS as a separate tracer aerosol species. A sensitivity run was performed with  
47 POA evaporation assuming that the modeled POA emissions had the volatility  
48 distribution described in Robinson et al. (2007). As an example, this corresponds to POA  
49 reductions by a factor of ~3.8 for dilution to ambient conditions at organic aerosol  
50 concentrations of 10  $\mu\text{g/m}^3$  and a temperature of 298 K. IVOC emissions were  
51 parameterized from the POA emissions in the NEIs, as in Robinson et al. (2007).

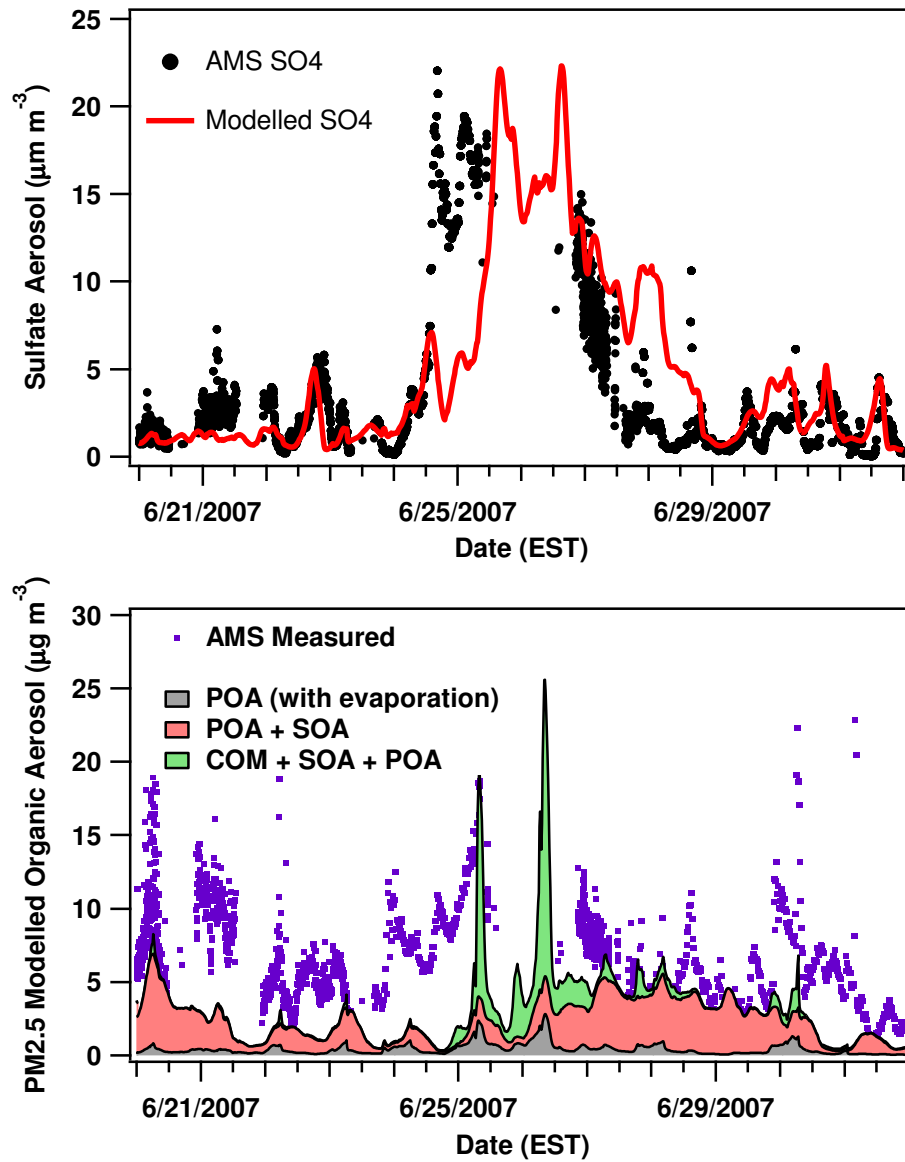
52 Biogenic emissions were calculated on-line by AURAMS using BEIS version  
53 3.09, the Biogenic Emissions Landcover Database (BELD3) vegetation data set (30 tree  
54 species, 20 crop species), and meteorological fields (temperature and irradiance) from  
55 GEM. Biogenic VOC emissions are speciated into four groups: isoprene; monoterpenes;  
56 sesquiterpenes; and "other VOCs". Monoterpene emissions for pine and spruce trees  
57 were updated based on recent satellite LAI retrievals and ground survey measurements of  
58 leaf area densities during the BOREAS field program in the Canadian boreal forest  
59 ([http://www.iwaqfr-2010.ca/presentations/Stroud\\_final\\_Emissions.ppt](http://www.iwaqfr-2010.ca/presentations/Stroud_final_Emissions.ppt)). Sesquiterpene  
60 emissions were calculated by scaling monoterpene emissions, as described in Helmig et  
61 al., (2007) (e.g., sesquiterpene emissions were a factor of 0.16 lower than monoterpenes  
62 at 30C).

63 The gas-phase mechanism in AURAMS is an updated version of the ADOM-II  
64 mechanism (Lurmann et al., 1986; Stockwell et al., 1989; Kuhn et al., 1998) that is solved  
65 using a vectorized version of the rodas3 solver (Sandu and Sander, 2006). A detailed  
66 description of the ADOM-II VOC lumping scheme can be found in Stroud et al. (2008).

67 In this study, a lumped monoterpene species was separated from the original ADOM-II  
68 anthropogenic long-chain alkene species and assigned the OH/O<sub>3</sub>/NO<sub>3</sub> kinetics of α-  
69 pinene. A lumped sesquiterpene species was added to the mechanism and modelled with  
70 β-caryophyllene OH/ O<sub>3</sub>/NO<sub>3</sub> kinetics. Benzene was separated from the original ADOM-  
71 II lumped species, propane (sum of propane, acetylene and benzene), and reacted in the  
72 modified mechanism with OH kinetics. The overall organic aerosol yield approach was  
73 applied to the following VOC precursor species: isoprene (ISOP), monoterpenes (PINE),  
74 sesquiterpenes (SESQ), benzene (BENZ), mono-substituted aromatics (TOLU), multi-  
75 substituted aromatics (AROM), long chain anthropogenic alkenes (ALKE), long chain  
76 anthropogenic alkanes (ALKA) and intermediate volatile organic compounds (IVOC).  
77 Aerosol yields were calculated for low and high NO<sub>x</sub> limits as a function of existing  
78 organic aerosol loadings (sum of primary and secondary) and temperature. Updated α<sub>i</sub>  
79 and K<sub>i</sub> values were based on recent literature studies (ISOP, Kroll et al. (2006) and Lane  
80 et al. (2008); PINE, Pathak et al. (2007), Griffin et al., (1999) and Zhang et al. (2006);  
81 SESQ, Lane et al. (2008); BENZ, Ng et al. (2006); TOLU, Hildebrandt et al. (2009);  
82 AROM, Ng et al. (2007); ALKE, Lane et al. (2008); and ALKA, Lane et al. (2008);  
83 IVOCs, Pye and Seinfeld, (2010)). An incremental increase in SOA mass was calculated  
84 from decreases in precursor VOC concentrations for a given time step under both low and  
85 high NO<sub>x</sub> conditions. A linear interpolation between the low NO<sub>x</sub> and high NO<sub>x</sub>  
86 incremental SOA mass was performed based on the fraction of the RO<sub>2</sub> radicals that  
87 react with HO<sub>x</sub> vs NO<sub>x</sub> (Presto and Donahue, 2006; Henze et al., 2008). An organic  
88 particle density of 1.5 g cm<sup>-3</sup> was assumed for conversion of normalized aerosol yield  
89 data. The particle size distribution is represented in the CTM by 12 size bins ranging  
90 from 0.01 to 40.96 μm in Stokes diameter, with the 8 lower bins corresponding to sizes  
91 below 2.5 μm. Particle composition is represented by nine chemical species (sulfate,  
92 nitrate, ammonium, black carbon, POA, SOA, crustal material, sea salt, and particulate  
93 water), which are assumed to be internally mixed within each size bin (14). Condensation  
94 of the SOA to the particle size distribution is described by a modified Fuchs-Sutugin  
95 equation as described by equation A14 in Gong et al. (2003).

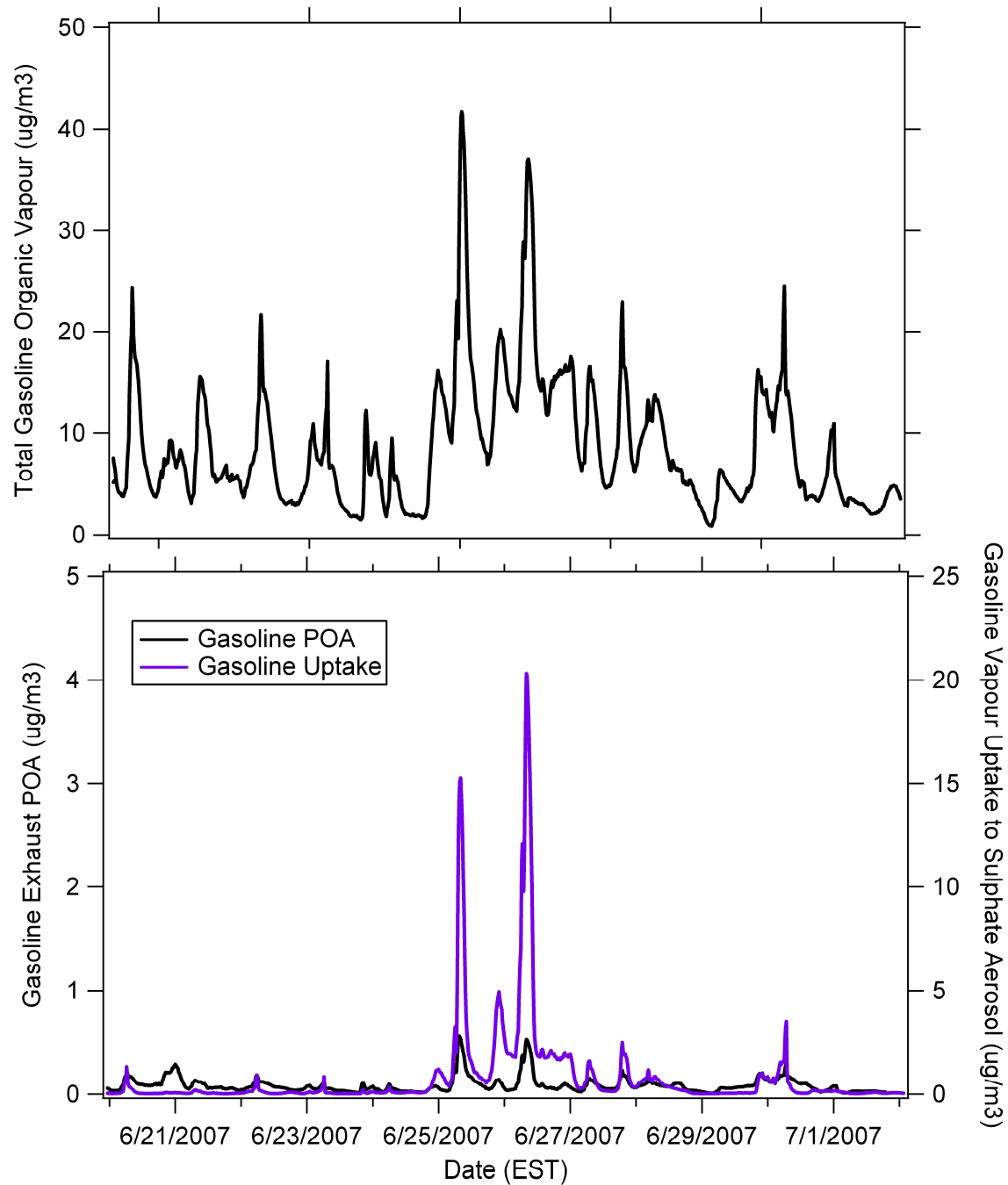
96           Figure S1 illustrates the model and measured time series at Windsor, ON for  
97 sulfate and organic aerosol. Sulfate is modeled reasonably well compared to the measured  
98 sulfate in terms of maximum for the 12 day period and diurnal cycles with the exception  
99 of the model underestimate for the afternoon on June 25 to the following afternoon on  
100 June 26. Panel b includes traces for POA (from the evaporation sensitivity run), SOA  
101 (traditional method with updated monoterpene emissions for pine and spruce trees) and  
102 the gasoline vapour uptake to sulfate aerosol. Good organic aerosol closure is achieved  
103 for the mid-morning June 25 maximum comparing the sum of the three modeled traces  
104 and the AMS organic aerosol measurements. Unfortunately, AMS data were missing for  
105 the June 26 modeled maximum. For other times, model organic aerosol predictions were  
106 still underpredicted. Figure S2 illustrates the gasoline vapour mixing ratio (panel a) and  
107 the gasoline exhaust POA compared to the gasoline vapour uptake to sulfate aerosol  
108 (panel b). The gasoline uptake to sulfate was considerably higher than the gasoline  
109 exhaust POA in the NEIs.

110



111  
 112  
 113  
 114

Figure S1. Windsor time series for measured and modelled sulphate aerosol (top panel) and organic aerosol (bottom panel, traces for POA, SOA, and COM stacked).



115  
 116  
 117  
 118  
 119  
 120  
 121

Figure S2. Windsor time series for total gasoline organic vapour (top panel), gasoline exhaust primary organic aerosol (bottom panel) and gasoline vapour uptake to sulphate aerosol (bottom panel).

122 References

123

124 Pye, H. O. T., and J. H. Seinfeld. 2010. A global perspective on aerosol from low-  
125 volatility organic compounds. *Atmospheric Chemistry and Physics* 10, (9): 4377-4401.

126

127 Gong, S. L., L. A. Barrie, J. -P Blanchet, K. von Salzen, U. Lohmann, G. Lesins, L.  
128 Spacek, et al. 2003. Canadian aerosol module: A size-segregated simulation of  
129 atmospheric aerosol processes for climate and air quality models 1. module development.  
130 *Journal of Geophysical Research D: Atmospheres* 108, (1): AAC 3-1 AAC 3-16

131

132 Griffin, R. J., D. R. Cocker III, R. C. Flagan, and J. H. Seinfeld. 1999. Organic aerosol  
133 formation from the oxidation of biogenic hydrocarbons. *Journal of Geophysical Research*  
134 *D: Atmospheres* 104, (D3): 3555-3567

135

136 Helmig, D., J. Ortega, T. Duhl, D. Tanner, A. Guenther, P. Harley, C. Wiedinmyer, J.  
137 Milford, and T. Sakulyanontvittaya. 2007. Sesquiterpene emissions from pine trees -  
138 identifications, emission rates and flux estimates for the contiguous united states.  
139 *Environmental Science and Technology* 41, (5): 1545-1553

140

141 Henze, D. K., J. H. Seinfeld, N. L. Ng, J. H. Kroll, T. -M Fu, D. J. Jacob, and C. L.  
142 Heald. 2008. Global modeling of secondary organic aerosol formation from aromatic  
143 hydrocarbons: High- vs. low-yield pathways. *Atmospheric Chemistry and Physics* 8, (9):  
144 2405-2421

145

146 Kroll, J. H., N. L. Ng, S. M. Murphy, R. C. Flagan, and J. H. Seinfeld. 2006. Secondary  
147 organic aerosol formation from isoprene photooxidation. *Environmental Science and*  
148 *Technology* 40, (6): 1869-1877

149

150 Kuhn, M., P. J. H. Builtjes, D. Poppe, D. Simpson, W. R. Stockwell, Y. Andersson-  
151 Sköld, A. Baart, et al. 1998. Intercomparison of the gas-phase chemistry in several  
152 chemistry and transport models. *Atmospheric Environment* 32, (4): 693-709

153

154 Lane, T. E., N. M. Donahue, and S. N. Pandis. 2008. Effect of NO<sub>x</sub> on secondary organic  
155 aerosol concentrations. *Environmental Science and Technology* 42, (16): 6022-6027

156

157 Lurmann, F. W., I. Loyd, A. C. and Atkinson, R. (1986) A chemical mechanism for use in  
158 long-range transport/acid deposition computer modeling. *Journal of Geophysical*  
159 *Research* 91, 10 905-10 936.

160

161 Ng, N. L., J. H. Kroll, A. W. H. Chan, P. S. Chhabra, R. C. Flagan, and J. H. Seinfeld.  
162 2007. Secondary organic aerosol formation from m-xylene, toluene, and benzene.  
163 *Atmospheric Chemistry and Physics* 7, (14): 3909-3922

164

165 Pathak, R. K., A. A. Presto, T. E. Lane, C. O. Stanier, N. M. Donahue, and S. N. Pandis.  
166 2007. Ozonolysis of  $\gamma$ -pinene: Parameterization of secondary organic aerosol mass  
167 fraction. *Atmospheric Chemistry and Physics* 7, (14): 3811-3821

168  
169 Presto, A. A., and N. M. Donahue. 2006. Investigation of  $\gamma$ -pinene + ozone secondary  
170 organic aerosol formation at low total aerosol mass. *Environmental Science and*  
171 *Technology* 40, (11): 3536-3543  
172  
173 Robinson, A. L., N. M. Donahue, M. K. Shrivastava, E. A. Weitkamp, A. M. Sage, A. P.  
174 Grieshop, et al. 2007. Rethinking organic aerosols: Semivolatile emissions and  
175 photochemical aging. *Science*, 315(5816), 1259-1262.  
176  
177 Sandu, A., and R. Sander. 2006. Technical note: Simulating chemical systems in  
178 Fortran90 and matlab with the kinetic PreProcessor KPP-2.1. *Atmospheric Chemistry and*  
179 *Physics* 6, (1): 187-195  
180  
181 Slowik, J.C., C. Stroud, J. W. Bottenheim, P. C. Brickell, R. Y.-W. Chang, J. Liggio,  
182 P. A. Makar, R. V. Martin, M. D. Moran, N. C. Shantz, S. J. Sjostedt, A. van Donkelaar,  
183 A. Vlasenko, H. A. Wiebe, A. G. Xia, J. Zhang, W. R. Leitch, and J. P. D. Abbatt, 2010.  
184 Characterization of a large biogenic secondary organic aerosol event from eastern  
185 Canadian forests, *Atmos. Chem. Phys.*, 10, 2825-2845.  
186  
187 Smyth, S. C., W. Jiang, H. Roth, M. D. Moran, P. A. Makar, F. Yang, V. S. Bouchet, and  
188 H. Landry. 2009. A comparative performance evaluation of the AURAMS and CMAQ  
189 air-quality modelling systems. *Atmospheric Environment* 43, (5): 1059-1070.  
190  
191 Stockwell, W.R., Lurmann, F.W., Intercomparison of the ADOM and RADM Gas-Phase  
192 Chemical Mechanisms, Electrical Power Research Institute Topical Report, 258 pp, 1989.  
193  
194 Stroud, C. A., G. Morneau, P. A. Makar, M. D. Moran, W. Gong, B. Pabla, J. Zhang, et  
195 al. 2008. OH-reactivity of volatile organic compounds at urban and rural sites across  
196 Canada: Evaluation of air quality model predictions using speciated VOC measurements.  
197 *Atmospheric Environment* 42, (33): 7746-7756  
198  
199 Zhang, J., K.E. Huff Hartz, S.N. Pandis, and N. M. Donahue. 2006. Secondary organic  
200 aerosol formation from limonene ozonolysis: Homogeneous and heterogeneous  
201 influences as a function of NO<sub>x</sub>. *Journal of Physical Chemistry A* 110, (38): 11053-  
202 11063